see related editorial on page 995

LIVER

Novel 3D Magnetic Resonance Elastography for the Noninvasive Diagnosis of Advanced Fibrosis in NAFLD: A Prospective Study

Rohit Loomba, MD, MHSc[1,2,3], Jeffrey Cui, MAS[2], Tanya Wolfson, MA[4], William Haufe, BS[5], Jonathan Hooker, BS[5], Nikolaus Szeverenyi, PhD[5], Brandon Ang, BS[2], Archana Bhatt, MS[2], Kang Wang, PhD, MAS[5], Hamed Aryafar, MD[6], Cindy Behling, MD[7], Mark A. Valasek, MD, PhD[8], Grace Y. Lin, MD, PhD[8], Anthony Gamst, PhD[4], David A. Brenner, MD[1], Meng Yin, PhD[9], Kevin J Glaser, PhD[9], Richard L. Ehman, MD[9] and Claude B. Sirlin, MD[5]

OBJECTIVES: **Recent studies show two-dimensional (2D)-magnetic resonance elastography (MRE) is accurate in diagnosing advanced fibrosis (stages 3 and 4) in nonalcoholic fatty liver disease (NAFLD) patients. Three-dimensional (3D)-MRE is a more advanced version of the technology that can image shear-wave fields in 3D of the entire liver. The aim of this study was to prospectively compare the diagnostic accuracy of 3D-MRE and 2D-MRE for diagnosing advanced fibrosis in patients with biopsy-proven NAFLD.**

METHODS: **This cross-sectional analysis of a prospective study included 100 consecutive patients (56% women) with biopsy-proven NAFLD who also underwent MRE. Area under the receiver operating characteristic (AUROC) analysis was performed to assess the accuracy of 2D- and 3D-MRE in diagnosing advanced fibrosis.**

RESULTS: **The mean (±s.d.) of age and body mass index were 50.2 (±13.6) years and 32.1 (±5.0) kg/m², respectively. The AUROC for diagnosing advanced fibrosis was 0.981 for 3D-MRE at 40 Hz, 0.927 for 3D-MRE at 60 Hz (standard shear-wave frequency), and 0.921 for 2D-MRE at 60 Hz (standard shear-wave frequency). At a threshold of 2.43 kPa, 3D-MRE at 40 Hz had sensitivity 1.0, specificity 0.94, positive predictive value 0.72, and negative predictive value 1.0 for diagnosing advanced fibrosis. 3D-MRE at 40 Hz had significantly higher AUROC (P<0.05) than 2D-MRE at 60 Hz for diagnosing advanced fibrosis.**

CONCLUSIONS: **Utilizing a prospective study design, we demonstrate that 3D MRE at 40 Hz has the highest diagnostic accuracy in diagnosing NAFLD advanced fibrosis. Both 2D- and 3D-MRE at 60 Hz, the standard shear-wave frequency, are also highly accurate in diagnosing NAFLD advanced fibrosis.**

Am J Gastroenterol 2016; 111:986–994; doi:10.1038/ajg.2016.65; published online 22 March 2016

INTRODUCTION

Nonalcoholic fatty liver disease (NAFLD) represents a spectrum of liver pathologies ranging from benign steatosis to nonalcoholic steatohepatitis (NASH) in patients with little to no prior history of alcohol consumption or secondary causes of hepatic steatosis (1,2). NAFLD is associated with components of the metabolic syndrome, including obesity, hypertriglyceridemia, and type 2 diabetes mellitus (3–6), and is now a prominent cause of liver disease in both the United States and worldwide (7–9). NAFLD patients with advanced fibrosis require monitoring and therapy due to their high risk for progression to cirrhosis and its complications, including portal hypertension, esophageal varices, and

[1]Division of Gastroenterology, Department of Medicine, University of California at San Diego, La Jolla, California, USA; [2]NAFLD Research Center, Department of Medicine, University of California at San Diego, La Jolla, California, USA; [3]Division of Epidemiology, Department of Family and Preventive Medicine, University of California at San Diego, La Jolla, California, USA; [4]Department of Mathematics, University of California at San Diego, La Jolla, California, USA; [5]Liver Imaging Group, Department of Radiology, University of California at San Diego, La Jolla, California, USA; [6]Department of Radiology, University of California at San Diego, La Jolla, California, USA; [7]Department of Pathology, Sharp Health System, San Diego, California, USA; [8]Department of Pathology, University of California at San Diego, La Jolla, California, USA; [9]Department of Radiology, Mayo Clinic, Rochester, Minnesota, USA. **Correspondence:** Rohit Loomba, MD, MHSc, NAFLD Research Center, Division of Gastroenterology, Department of Medicine, University of California at San Diego, La Jolla, California 92093-0063, USA or Claude B. Sirlin, MD, Liver Imaging Group, Department of Radiology, University of California at San Diego, 408 Dickinson Street, San Diego, California 92103-8226, USA. E-mail: roloomba@ucsd.edu or csirlin@ucsd.edu
Received 9 October 2015; accepted 10 February 2016

hepatocellular carcinoma (10–13). Biopsy is currently the gold standard for advanced fibrosis diagnosis in NAFLD patients, but is invasive, has high inter-observer variability, and is associated with adverse side effects including bleeding, pain, and even death (14,15). There is a strong need for the noninvasive diagnosis of advanced fibrosis in NAFLD patients.

There is a well-established need for accurate, noninvasive, and commercially available tests to diagnose NAFLD-associated advanced fibrosis. Noninvasive markers such as Cytokeratin-18 (ref. 16), NAFLD fibrosis score (17), FIB-4 (ref. 18), and Enhanced Liver Fibrosis (19) may not be accurate enough for routine clinical use in all patients (1,20,21). Ultrasound-based methods, including acoustic radiation force impulse imaging and transient elastography (FibroScan), have high (21–50%) failure rates in NAFLD patients (22–25). Magnetic resonance elastography (MRE) is a novel magnetic resonance technique utilizing shear waves to characterize liver fibrosis. A special magnetic resonance imaging (MRI) technique is used to image propagating mechanical waves in tissue and these images are processed with an algorithm to generate cross-sectional images that quantitatively depict tissue stiffness. In general, it is necessary to image the pattern of propagating waves in three dimensions (3D) in order to properly calculate tissue stiffness. However, commercial implementations of hepatic MRE that are currently available use hardware designed to generate mechanical waves that propagate transversely in the liver and special processing algorithms that allow valid stiffness measurements to be obtained using single two-dimensional (2D) axial images of the wave pattern. Two-dimensional MRE (2D-MRE) is less demanding from an instrumentation standpoint than 3D-MRE and is the approach that is currently used in commercially available versions of MRE because it can be easily implemented on basic MRI systems. 2D-MRE has been prospectively shown to be highly accurate for advanced fibrosis diagnosis (26–28). Although technically more demanding, 3D-MRE offers advantages that might provide even higher diagnostic performance.

Utilizing a *prospective* study design, we compared the accuracy of 3D-MRE and 2D-MRE for diagnosing advanced fibrosis in a cohort of patients with biopsy-confirmed NAFLD. We also compared the accuracy of 3D-MRE and 2D-MRE for diagnosing other stages of fibrosis in NAFLD patients and for diagnosing NASH.

METHODS

Design

This is a cross-sectional analysis of a prospective cohort consisting of 100 consecutive patients with biopsy-proven NAFLD who underwent 2D-MRE and 3D-MRE imaging. Liver biopsies were obtained for clinical care and MRIs were obtained for research. After undergoing careful exclusion for other causes of liver diseases and secondary causes of hepatic steatosis, patients attended a research clinic visit for standardized history, physical exam, anthropometric exam, and biochemical testing at the University of California at San Diego (UCSD) NAFLD Translational Research Unit (29–33) and an imaging visit at the UCSD MR3T Research Laboratory for 2D- and 3D-MRE. Informed consent was obtained from all patients. This study was approved by the UCSD Institutional Review Board and the UCSD Clinical and Translational Research Institute.

Inclusion/exclusion criteria

Patients ≥18 years old with biopsy-confirmed NAFLD and written informed consent who did not meet any exclusion criteria were included in the study. Exclusion criteria included: regular and excessive alcohol consumption within 2 years of recruitment (≥14 drinks/week for men or ≥7 drinks/week for women), use of hepatotoxic drugs or drugs known to cause hepatic steatosis, clinical or laboratory evidence of secondary NAFLD due to major nutritional and iatrogenic gastrointestinal disorders or HIV infection, liver diseases other than NAFLD, including viral hepatitis (detected with positive serum hepatitis B surface antigen or hepatitis C viral RNA), Wilson's disease, hemochromatosis, glycogen storage disease, alpha-1 antitrypsin deficiency, autoimmune hepatitis, and cholestatic or vascular liver disease, clinical or biochemical evidence of decompensated liver disease (Child-Pugh score >7 points), evidence of active substance abuse, significant systemic illnesses, contraindication(s) to MRI, pregnant or trying to become pregnant, or any other condition which, in the investigator's opinion, may affect the patient's competence or compliance in completing the study.

Clinical research assessment

All patients received clinical assessments at the UCSD NAFLD Research Center. A detailed history was obtained from all patients. A physical exam, which included vital signs, height, weight, and anthropometric measurements, was performed by a trained clinical investigator. Body mass index was defined as the body weight (in kilograms) divided by height (in meters) squared. Alcohol consumption was documented in outside clinical visits and confirmed in the research clinic using the Alcohol Use Disorders Identifications Test and the Skinner questionnaire, both of which are validated tools to screen for heavy drinking and/or active alcohol abuse or dependence. A detailed history of medications was obtained and no patient took medications known or suspected to cause steatosis or steatohepatitis. Other causes of liver disease were systemically ruled out using detailed history and laboratory data. Subjects underwent the following biochemical tests: aspartate aminotransferase, alanine aminotransferase, alkaline phosphatase, gamma-glutamyl transpeptidase, total bilirubin, direct bilirubin, albumin, hemoglobin A1c, fasting glucose, insulin, homeostatic model assessment of insulin resistance, prothrombin time, international normalized ratio, fasting lipid panel, free fatty acids, C-reactive protein, and platelet count. homeostatic model assessment of insulin resistance was defined as the product of glucose and insulin divided by 405.

Histologic assessment

All patients underwent a systemic liver biopsy evaluation by an experienced liver pathologist blinded to the patients' laboratory and radiologic data. The Nonalcoholic Steatohepatitis Clinical Research Network (NASH CRN) histological scoring system (34)

© 2016 by the American College of Gastroenterology

was used for this study. Hepatic fibrosis was scored on a five-point scale (0, 1, 2, 3, 4), with advanced fibrosis defined as stage 3–4 fibrosis. Hepatic steatosis and lobular inflammation were scored on four-point scales (0, 1, 2, 3) and hepatic ballooning was scored on a three-point scale (0, 1, 2). The NAFLD activity score (NAS score) was the sum of the steatosis, lobular inflammation, and ballooning scores and ranged from 0 to 8. NASH was scored on a three-point scale (non-NASH, borderline NASH, and definite NASH). Patients with both borderline NASH and definite NASH were classified as having NASH for the purpose of this study. The average (±s.d.) of biopsy size and number of portal triads was 23.2 (±9.5) mm and 13.7 (±5.9) mm, respectively. 10/100 (10%) of the cohort had biopsy lengths shorter than 15 mm.

Outcome measures

The primary outcome was advanced fibrosis (stage 3 and 4 fibrosis). The secondary outcomes were the remaining dichotomized fibrosis stages: stage 0 vs. stage 1–4 fibrosis, stage 0–1 vs. stage 2–4 fibrosis, and stage 0–3 vs. stage 4 fibrosis.

Magnetic resonance imaging

MRI was performed using a 3T research scanner (GE Signa EXCITE HDxt; GE Healthcare, Waukesha, WI). Patients were instructed to fast for at least four hours before exam to reduce potential physiologic confounding factors. MRE was performed to assess hepatic stiffness.

Magnetic resonance elastography

MRE was performed with a modified advanced version of 2D-MRE similar to the commercially available "MR-touch" product from GE Healthcare and a prototype 3D-MRE implementation developed at the Mayo Clinic (27,35–38).

MRE data acquisition

2D- and 3D-MRE were performed using the standard shear-wave frequency of 60 Hz used in commercial versions of the technique. 3D-MRE data were also obtained using a shear-wave frequency of 40 Hz. The exams were performed as previously described in the literature (35,36). A device for applying mechanical vibrations during scanning was applied to the body wall anterior to the liver and held in place with an elastic belt. Total imaging time for 2D- and 3D-MRE at 60 Hz and 3D-MRE at 40 Hz was less than 3.5 min. 2D-MRE was performed at a driver frequency of 60 Hz. A motion-sensitized gradient-recalled-echo imaging sequence was performed at four different phase offsets during one 16-s breath hold. This was repeated at four separate axial slices (10 mm thick, 10 mm interslice gap) at the widest transverse section of the liver with short recovery in between. Acquisition parameters for each axial slice were as follows: 1 motion-sensitizing direction (superior to inferior); repetition time, 50 ms; echo time, 20.2 ms; flip angle (FA), 30°; matrix, 256×64; field of view, 38×38 cm^2; one-signal average; receiver bandwidth ±31.25 kHz; and parallel imaging acceleration factor, 2.

3D-MRE was performed separately at 40 and 60 Hz driver frequencies. For each exam, a separate motion-sensitized, multi-slice, spin-echo echo-planar-imaging sequence was performed to capture shear-wave displacements along the *x*-, *y*-, and *z*-directions for a single phase-offset. Data acquisition for the three sets of wave data was performed during one 21-s breath-hold scan, and then repeated at three different phase offsets. The acquisition parameters for both 40 and 60 Hz, at each phase offset, were as follows: 32 axial slices covering most of the liver, 3.5 mm thick; repetition time, 1,200 (1,333.8) ms; echo time, 37.1 (49.4) ms; FA, 90°; matrix, 72×72; field of view, 44.8×44.8 cm^2; receiver bandwidth ±250 kHz; and parallel imaging acceleration factor, 3.

MRE processing

For 2D-MRE, processing was automatically performed on the imager using the same algorithm that is used in commercial implementations of the technology, producing liver stiffness maps (called elastograms) (39). These maps display the spatial distribution of a stiffness parameter called the magnitude of the complex shear modulus. For 3D-MRE, a prototype 3D direct inversion algorithm with characteristics similar to the 2D algorithm was used.

Elastograms were transferred offline for analysis (40,41) by a trained image analyst with at least 6 months of experience working with MRE. The image analyst drew regions of interest on the elastograms, including only liver parenchyma while avoiding liver edges, large blood vessels, and artifacts. The per-pixel stiffness values across regions of interest were calculated and automatically outputted to an electronic spreadsheet.

Duration between MRE and liver biopsy

The median (interquartile range) time interval between MRE and biopsy was 46 (44) days.

Statistical analyses

An experienced biostatistical analyst (T.W.) performed the statistical analyses for this study under the supervision of a faculty statistician (A.G.) using "R" statistical computing software (R version 2.15.1 [2012–06–22]; R: a language and environment for statistical computing; R Foundation for Statistical Computing, Vienna, Austria). Demographic, laboratory, histological, and imaging data were summarized using mean and standard deviation for continuous measures and counts and percentages for categorical measures. A two-tailed *P*-value ≤0.05 was considered statistically significant.

Main analysis and cross-validation

Receiver operating characteristic (ROC) curve analysis was performed to assess the utility of 3D-MRE at 40 and 60 Hz and 2D-MRE at 60 Hz for diagnosing advanced fibrosis (stage 3–4 fibrosis). The area under ROC curves (AUROCs) were calculated for 3D-MRE and 2D-MRE. The cutoff value needed to obtain a minimum specificity of 0.9 was determined, and the following performance parameters were calculated: sensitivity, specificity, positive predictive value (PPV), and negative predictive valve (NPV). Sixfold cross-validation was performed on the threshold selection method for 3D-MRE and 2D-MRE and the same performance parameters were calculated. 95% Confidence

intervals (CIs) were calculated for both raw and cross-validated performance parameters. Bootstrap-based comparisons were used to compare the AUROC of 3D-MRE at 40 and 60 Hz against the AUROC of 2D-MRE at 60 Hz.

Secondary analyses

Additional ROC analysis was performed to determine the AUROC, classifying threshold, performance parameter with 95% CIs, and cross-validated performance parameters for other diagnostic end points: any fibrosis (stage 0 vs. 1–4), mild fibrosis (stage 0–1 vs. 2–4), moderate fibrosis (stage 0–2 vs. 3–4), and cirrhosis (stage 0–3 vs. 4). The aspartate aminotransferase to Platelet Ratio Index (APRI) score was calculated using previously published formula (42) and the AUROCs of APRI vs. MRE was compared using the DeLong test (43).

RESULTS

Baseline characteristics

One hundred consecutive patients with biopsy-proven NAFLD and MRE were prospectively enrolled. The mean (±s.d.) of age and body mass index was 50.2 (±13.6) and 32.1 (±5.0), respectively. Baseline characteristics, including demographical, biochemical, histological, and imaging data, are summarized in **Table 1**. A total of 163 patients were observed at the NAFLD Translational Unit, although 63 were excluded because 3D-MRE and/or 2D-MRE were not performed. In our cohort of 100 patients, 2D-MRE (60 Hz), 3D-MRE (60 Hz), and 3D-MRE (40 Hz) were not obtained in 1, 2, and 8 patients, respectively, due to patient schedule.

Distribution of fibrosis stage

In all, 41, 32, 12, 10, and 5 patients had stage 0, 1, 2, 3, and 4 fibrosis, respectively. A total of 15 out of 100 patients (15.0% of total) had advanced fibrosis.

Accuracy of 2D-MRE for assessing advanced fibrosis

The AUROC for distinguishing advanced fibrosis from stage 0–2 fibrosis was 0.921 (P<0.0001; **Figure 1a**). At a raw threshold of 3.80 kPa (**Figure 2a**), 2D-MRE (60 Hz) had sensitivity of 0.867 (95% CI: 0.595–0.983), specificity of 0.940 (95% CI: 0.867–0.980), PPV of 0.722 (95% CI: 0.465–0.903), and NPV of 0.975 (95% CI: 0.914–0.997; **Table 2**). 2D-MRE (60 Hz) misclassified 5 out of 84 patients without advanced fibrosis and 2 out of 15 patients with advanced fibrosis.

Accuracy of 3D-MRE

As shown in **Figure 1b**, the AUROC for distinguishing advanced fibrosis from stage 0–2 fibrosis for 3D-MRE (60 Hz) is 0.927 (P<0.0001). At a raw threshold of 3.40 kPa (**Figure 2b**), 3D-MRE (60 Hz) had sensitivity of 0.867 (95% CI: 0.595–0.983), specificity of 0.964 (95% CI: 0.898–0.992), PPV of 0.812 (95% CI: 0.544–0.960), and NPV of 0.976 (95% CI: 0.915–0.997; **Table 2**). 3D-MRE (60 Hz) misclassified 3 out of 83 patients without advanced fibrosis and 2 out of 15 patients with advanced fibrosis.

Table 1. Baseline demographic, biochemical, and histological characteristics of study participants

	Patients with biopsy, 2D-MRE, and 3D-MRE (n=100)
Demographic	
Female patients (%)	56 (56%)
Age at biopsy (s.d.)	50.2 (13.6)
Height (m), mean (s.d.)	168.0 (10.7)
Weight (kg), mean (s.d.)	90.9 (17.9)
BMI (kg/m^2), mean (s.d.)	32.1 (5.0)
Ethnic origin	
White (%)	46 (46%)
African American (%)	1 (1%)
Asian (%)	17 (17%)
Hispanic (%)	32 (32%)
Multi-racial (%)	1 (1%)
Other (%)	1 (1%)
Refused to disclose (%)	2 (2%)
Diabetes (%)	33 (33%)
Biochemical profile	
AST (U/l), mean (s.d.)	46.5 (36.6)
ALT (U/l), mean (s.d.)	68.7 (57.5)
AST/ALT ratio mean (s.d.)	0.75 (0.30)
Alk Phos (U/l), mean (s.d.)	74.5 (23.4)
GGT (U/l), mean (s.d.)	66.4 (55.1)
Total bilirubin (mg/dl), mean (s.d.)	0.54 (0.38)
Direct bilirubin (mg/dl), mean (s.d.)	0.13 (0.08)
Albumin (g/dl), mean (s.d.)	4.5 (0.3)
Glucose (mg/dl), mean (s.d.)	108.1 (32.1)
Hgb A1C, mean (s.d.)	6.1 (0.9)
Triglycerides (mg/dl), mean (s.d.)	157.7 (76.6)
Total cholesterol (mg/dl), mean (s.d.)	184.0 (36.4)
HDL (mg/dl), mean (s.d.)	48.8 (15.7)
LDL (mg/dl), mean (s.d.)	103.9 (31.9)
Platelet count (10^9/l), mean (s.d.)	242.9 (73.8)
Protime mean (s.d.)	10.9 (1.0)
INR mean (s.d.)	1.0 (0.1)
Histology	
Steatosis	
1	33 (33%)
2	37 (37%)
3	30 (30%)
Lobular inflammation	
0	1 (1%)
1	40 (40%)

Table 1 continued on following page

© 2016 by the American College of Gastroenterology

Table 1. Continued

	Patients with biopsy, 2D-MRE, and 3D-MRE (*n*=100)
2	55 (55%)
3	4 (4%)
Ballooning	
0	24 (24%)
1	46 (46%)
2	30 (30%)
Fibrosis	
0	41 (41%)
1	32 (32%)
2	12 (12%)
3	10 (10%)
4	5 (5%)
NASH	
NAFLD, not NASH (%)	13 (13%)
Borderline NASH (%)	15 (15%)
Definite NASH (%)	72 (72%)
NAS mean (s.d.)	4.65 (1.47)
Imaging	
2D-MRE at 60 Hz mean (s.d.)	3.26 (1.28)
3D-MRE at 60 Hz mean (s.d.)	2.69 (1.13)
3D-MRE at 40 Hz mean (s.d.)	2.03 (0.96)

Alk phos, alkaline phosphatase; ALT, alanine aminotransferase; AST, aspartate aminotransferase; BMI, body mass index; GGT, gamma-glutamyl transpeptidase; HDL, high-density lipoprotein; Hgb A1c, hemoglobin A1c; LDL, low-density lipoprotein; INR, international normalized ratio; MRE, magnetic resonance elastography; NASH, nonalcoholic steatohepatitis; NAFLD, nonalcoholic fatty liver disease; NAS, nonalcoholic fatty liver disease activity score; 2D, two-dimensional; 3D, three-dimensional.

Accuracy of 3D-MRE at 40 Hz

As shown in **Figure 1c**, the AUROC for distinguishing advanced fibrosis from stage 0–2 fibrosis was 0.981 (P<0.0001) for 3D-MRE (40 Hz). At a raw threshold of 2.43 kPa (**Figure 2c**), 3D-MRE (40 Hz) had sensitivity of 1.0 (95% CI: 0.753–1.0), specificity of 0.937 (95% CI: 0.858–0.979), PPV of 0.722 (95% CI: 0.465, 0.903), and NPV of 1.0 (95% CI: 0.951–1.0; **Table 2**). 3D-MRE (40 Hz) misclassified 5 out of 79 patients without advanced fibrosis but correctly classified 13 out of 13 patients with advanced fibrosis.

Cross-validated 2D and 3D-MRE for advanced fibrosis diagnosis

Stratified sixfold cross-validation was performed for 2D-MRE and 3D-MRE in diagnosing advanced fibrosis. The sensitivity, specificity, PPV, and NPV of the cross-validated models were similar to that of the raw models (**Table 2**).

Comparison of 2D-MRE vs. 3D-MRE for advanced fibrosis diagnosis

In bootstrap-based comparisons, there were no significant difference in diagnostic performance, as assessed by the AUROC, between 2D-MRE (60 Hz) and 3D-MRE (60 Hz; 95% CI: −0.004 to 0.259). 3D-MRE (40 Hz) had higher AUROC than 2D-MRE (60 Hz) for diagnosing advanced fibrosis (95% CI: 0.001–0.223, P<0.05; **Figure 3**). Representative elastograms and biopsy slides of a patient with stage 4 fibrosis (cirrhosis) are shown for 2D-MRE (60 Hz), 3D-MRE (40 Hz), and 3D-MRE (60 Hz; **Figure 4**).

3D- and 2D-MRE for diagnosis of other fibrosis stages and NASH

The accuracy of 3D- and 2D-MRE for discriminating other stages of liver fibrosis, with the estimated cutoffs, is summarized in **Table 3**. MRE had AUROCs of 0.981, 0.983, and 0.993 for

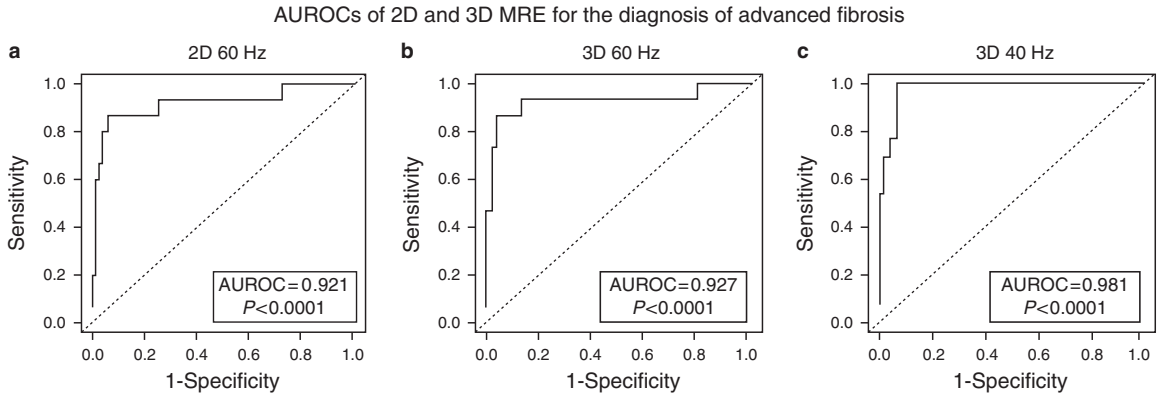

Figure 1. Area under receiver operating characteristic curves (AUROCs) of two-dimensional (2D)-magnetic resonance elastography (MRE) and three-dimensional (3D)-MRE for diagnosing advanced fibrosis. (**a**–**c**) The AUROC of 2D-MRE (60 Hz), 3D-MRE (60 Hz), and 3D-MRE (40 Hz) for diagnosing advanced fibrosis. 2D-MRE (60 Hz) had AUROC of 0.921, 3D-MRE (60 Hz) had AUROC of 0.927, and 3D-MRE (40 Hz) had AUROC of 0.981 for diagnosing advanced fibrosis.

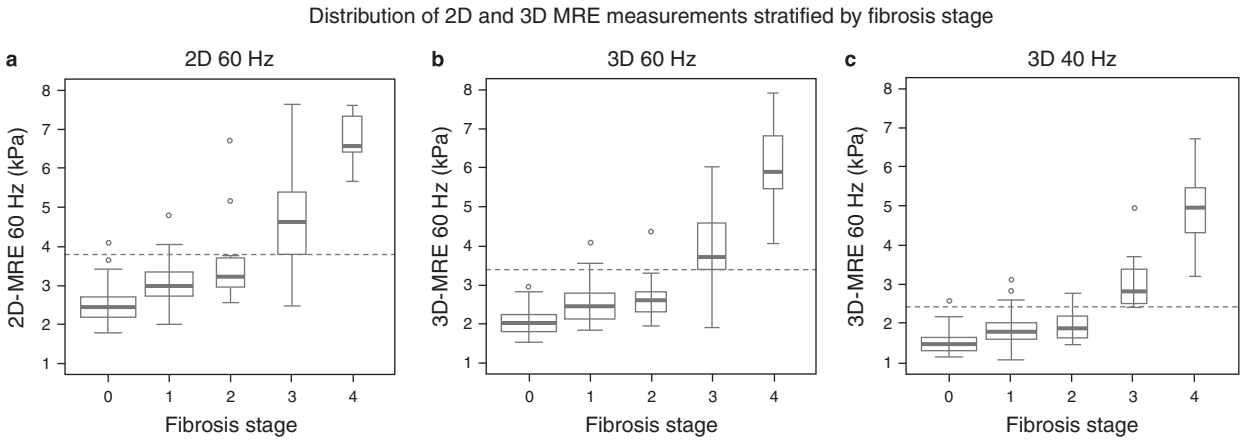

Figure 2. Distribution of two-dimensional (2D)- and three-dimensional (3D)- magnetic resonance elastography (MRE) measurements stratified by fibrosis stage. (**a**–**c**) The distribution of 2D- and 3D-MRE measurements stratified by fibrosis stage and the diagnostic threshold of 2D-MRE (60 Hz), 3D-MRE (60 Hz), and 3D-MRE (40 Hz) for diagnosing advanced fibrosis. 2D-MRE (60 Hz) predicted advanced fibrosis at threshold of 3.80 kPa, 3D-MRE (60 Hz) predicted advanced fibrosis at threshold of 3.40 kPa, and 3D-MRE (40 Hz) predicted advanced fibrosis at threshold of 2.43 kPa.

Table 2. Diagnostic test characteristics of 3D- and 2D-MRE for the detection of advanced fibrosis

	Biopsy		Number of MRE performed	AUROC	Cutoff (kPa)	Raw Sens	Raw Spec	Raw PPV	Raw NPV	CV Sens	CV Spec	CV PPV	CV NPV
	Advanced fibrosis	No advanced fibrosis											
2D-MRE (60 Hz)	15	85	99	0.921	3.80	0.867	0.940	0.722	0.975	0.800	0.952	0.750	0.964
3D-MRE (60 Hz)			98	0.927	3.40	0.867	0.964	0.812	0.976	0.800	0.964	0.800	0.964
3D-MRE (40 Hz)			92	0.981	2.43	1.000	0.937	0.722	1.000	0.923	0.937	0.706	0.987

AUROC, area under receiver operating characteristic curve; CV, cross-validated; MRE, magnetic resonance elastography; NPV, negative predictive value; PPV, positive predictive value; sens, sensitivity; spec, specificity; 2D, two-dimensional; 3D, three-dimensional.

diagnosing cirrhosis using 2D-MRE (60 Hz), 3D-MRE (60 Hz), and 3D-MRE (40 Hz), respectively. MRE had AUROCs of 0.754, 0.757, and 0.736 for diagnosing definite NASH using 2D-MRE (60 Hz), 3D-MRE (60 Hz), and 3D-MRE (40 Hz), respectively.

Comparison of MRE and APRI for diagnosis of advanced fibrosis

The AUROC of APRI for diagnosing advanced fibrosis was 0.719 (P=0.007). In direct comparisons of AUROCs using the DeLong test, 2D-MRE (60 Hz), 3D-MRE (60 Hz), and 3D-MRE (40 Hz) all had significantly higher AUROCs than APRI for diagnosing advanced fibrosis, with P-values of 0.018, 0.017, and <0.001, respectively.

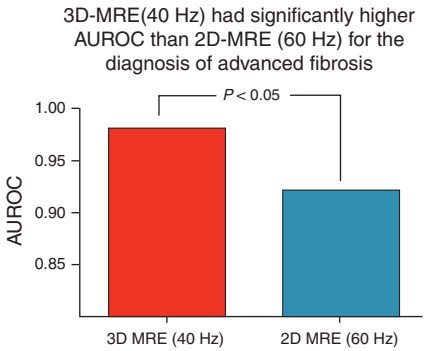

Figure 3. Three-dimensional (3D)-magnetic resonance elastography (MRE; 40 Hz) had significantly higher area under receiver operating characteristic curve (AUROC) than 2D-MRE (60 Hz) for the diagnosis of advanced fibrosis.

DISCUSSION

Main findings

Using a prospective cohort design of 100 patients, this study demonstrated that both 2D-MRE and 3D-MRE are highly accurate for diagnosing advanced fibrosis in patients with biopsy-proven NAFLD. 2D- and 3D-MRE are also highly accurate for the diagnosis of NAFLD-associated cirrhosis. In a head-to-head comparison, 3D-MRE at 40 Hz is significantly better than 2D-MRE at 60 Hz for advanced fibrosis detection. In this study, the diagnostic performance obtained with a shear wave frequency of 40 Hz was slightly higher than at 60 Hz.

© 2016 by the American College of Gastroenterology

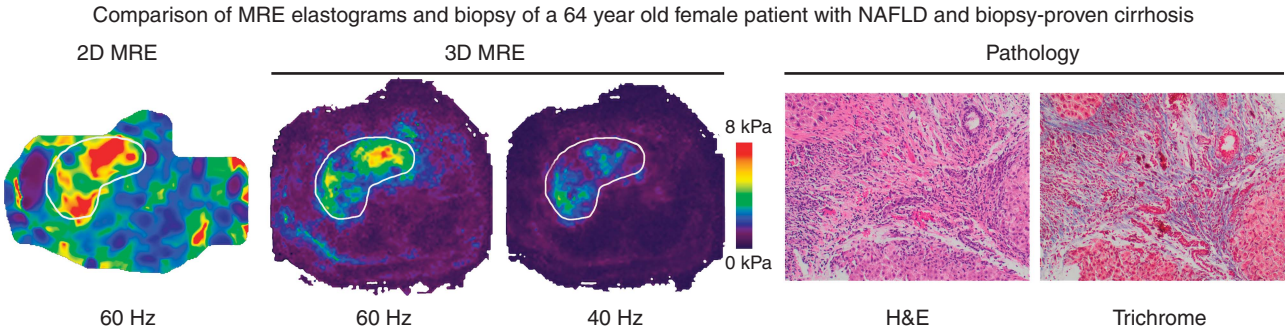

Figure 4. Comparison of magnetic resonance elastography (MRE) elastograms and biopsy stains of a 64-year-old female patient with nonalcoholic fatty liver disease (NAFLD) and biopsy-proven stage 4 fibrosis (cirrhosis). Patient had aspartate aminotransferase 59, alanine aminotransferase 34, alkaline phosphatase 113, total bilirubin 2.2, albumin 3.9, platelet count 91, and international normalized ratio 1.2 at time of biopsy and imaging. MRE was obtained at frequencies of 2D (60 Hz), 3D (60 Hz), and 3D (40 Hz). Biopsy was stained using hematoxylin and eosin (H&E) and trichrome stains and shows circumferential fibrosis and regenerative hepatocyte nodules consistent with cirrhosis.

Table 3. AUROC and diagnostic cutoffs of 3D- and 2D-MRE for the detection of different stages of fibrosis and NASH

	Primary outcome		Secondary outcomes							
	Stage 3–4 vs. stage 0–2	Cutoff (kPa)	Stage 1–4 vs. stage 0	Cutoff (kPa)	Stage 2–4 vs. stage 0–1	Cutoff (kPa)	Stage 4 vs. stage 0–3	Cutoff (kPa)	NASH vs. no NASH	Cutoff (kPa)
2D-MRE (60 Hz)	0.921	3.80	0.854	3.13	0.878	3.65	0.981	5.68	0.754	2.92
3D-MRE (60 Hz)	0.927	3.40	0.855	2.53	0.840	2.89	0.983	4.08	0.757	2.42
3D-MRE (40 Hz)	0.981	2.43	0.848	1.77	0.856	2.38	0.993	3.21	0.736	1.93

AUROC, area under receiver operating characteristic curve; MRE, magnetic resonance elastography; NASH, nonalcoholic steatohepatitis; 2D, two-dimensional; 3D, three-dimensional.

The non-invasive diagnosis of advanced fibrosis in NAFLD patients remains a major unmet need. Compared with 2D-MRE, 3D-MRE allows for improved assessment of spatial patterns of hepatic fibrosis and focal lesions. However, 2D-MRE is simpler to implement compared with 3D-MRE. This study shows that using the standard shear-wave frequency of 60 Hz, both 2D- and 3D-MRE have equivalent diagnostic performance and are highly effective in screening for advanced fibrosis in NAFLD patients. We propose that MRE is an accurate diagnostic test for the non-invasive diagnosis of advanced fibrosis and cirrhosis in NAFLD patients, and that both 2D- and 3D-MRE are highly effective for this purpose.

In context of published literature

This is the first prospective study to evaluate the diagnostic utility of 3D-MRE for diagnosing advanced fibrosis in NAFLD patients. It shows 3D-MRE to be highly accurate for diagnosing advanced fibrosis. This study is consistent with previous studies showing 2D-MRE to also be highly accurate for advanced fibrosis diagnosis in NAFLD patients (27,28). Although ultrasound-based imaging techniques may be useful for assessing hepatic fat volume in NAFLD patients (44), their utility in assessing advanced fibrosis is limited due to their high unreliable rates in obese patients (1,22–25,45,46). This may be problematic given the high prevalence of obesity in NAFLD patients (3,5–7). The diagnostic accuracy of MRE does not appear to be impacted by obesity or liver fat content (28,35). However, magnetic resonance technology is contraindicated in some patients, such as those with implanted electronic devices such as pacemakers or claustrophobia, and other imaging techniques may need to be pursued in these patients instead for noninvasive advanced fibrosis diagnosis (47).

Clinical prediction rules, including the NAFLD fibrosis score (17), FIB-4 (ref. 18), and APRI (42) may be used to predict advanced fibrosis in NAFLD patients (1,20,21,48). However, these clinical prediction rules have less diagnostic accuracy than MRE (48) and may have indeterminate ranges, and more accurate tests are needed. Although a low clinical prediction rule cutoff may be used to rule out advanced fibrosis and a high cutoff to rule in advanced fibrosis in NAFLD patients, 3D-MRE may provide additional diagnostic utility in patients with indeterminate clinical prediction rule scores.

Strengths and limitations

The strength of this study lies in its use of a prospective, well-characterized cohort of NAFLD patients with clinical indications for liver biopsy. The study was performed by experienced clinical investigators in a specialized NAFLD translational research unit for both clinical and radiologic research in NAFLD, and patients

were carefully excluded for other causes of liver disease before enrolling in the study. There is a short time interval (46 days) between biopsy and imaging. Liver biopsy, the gold standard for this study, was scored using the NASH CRN histological scoring system, which is well-validated for use in NAFLD patients. This is the first prospective study of biopsy-proven NAFLD that compares 3D-MRE vs. 2D-MRE in a large cohort of uniquely well-characterized patients.

However, we acknowledge following limitations. It is a cross-sectional analysis of a prospective cohort and does not longitudinally look at changes in fibrosis over time. The diagnostic accuracy of 3D- and 2D-MRE was compared with biopsy, which may be prone to sampling variability. Since the study was performed at a single center skilled in working with NAFLD patients, its generalizability in other clinical settings is unknown. The cost-effectiveness of 3D-MRE compared with 2D-MRE and biopsy is also unknown, although at our center MRE is cheaper to perform than biopsy without the associated morbidity and mortality. MRE may be contraindicated in some patients, such as those with metal implants or claustrophobia, thus potentially limiting its use in some NAFLD patients.

Impact on future research

This study demonstrates both 2D- and 3D-MRE are highly accurate for advanced fibrosis diagnosis in a prospective cohort of patients with biopsy-proven NAFLD. The evidence that MRE performed at a lower shear-wave frequency of 40 Hz may provide increased diagnostic performance provides motivation for further investigation of this issue.

In summary, this study provides evidence that the diagnostic performance of 2D-MRE, which is technically undemanding, is similar to that of full 3D wave field MRE in noninvasive screening of NAFLD-associated advanced fibrosis in a community setting. Further multicenter studies are needed to evaluate the utility of 2D- and 3D-MRE for monitoring longitudinal changes in liver fibrosis in both natural history studies and intervention trials. The cost-effectiveness of utilizing 3D-MRE compared with 2D-MRE and/or biopsy must also be evaluated to devise comprehensive, cost-efficient screening strategies for NAFLD-associated advanced fibrosis.

CONFLICT OF INTEREST

Guarantors of the article: Rohit Loomba, MD, MHSc and Claude B. Sirlin, MD.

Specific author contributions: Rohit Loomba and Claude B. Sirlin—study concept and design, analysis and interpretation of data, drafting of the manuscript, critical revision of the manuscript, obtained funding, study supervision, approved final submission. Jeffrey Cui and Tanya Wolfson—analysis and interpretation of data, statistical analysis, drafting of the manuscript, critical revision of the manuscript, approved final submission. William Haufe, Jonathan Hooker, Brandon Ang and Archana Bhatt—data collection, critical revision of the manuscript, approved final submission. Nikolaus Szeverneyi—MRE procedures, critical revision of the manuscript, approved final submission. Kang Wang—drafting of the manuscript, critical revision of the manuscript, approved final submission. Hamed Aryafar—data collection, interpretation of data, critical revision of the manuscript, approved final submission. Cindy Behling and Mark A. Valasek—critical revision of the manuscript, approved final submission. Grace Y. Lin and David A. Brenner—critical revision of the manuscript, approved final submission. Anthony Gamst—statistical analysis, critical revision of the manuscript, approved final submission. Meng Yin and Richard L. Ehman—MRE procedures, critical revision of the manuscript, approved final submission. Kevin J. Glaser—MRE data analysis, critical revision of the manuscript, approved final submission.

Funding support: The study was conducted at the Clinical and Translational Research Institute, University of California at San Diego. R.L. is supported in part by the American Gastroenterological Association (AGA) Foundation—Sucampo—ASP Designated Research Award in Geriatric Gastroenterology and by a T. Franklin Williams Scholarship Award; Funding provided by: Atlantic Philanthropies, Inc, the John A. Hartford Foundation, the Association of Specialty Professors, and the American Gastroenterological Association and grant K23-DK090303. J.C. is supported by NIH T32 training grant 5TL1TR000098. Additional funding provided by R01DK088925 (PI-CS) and NIH grant EB001981 (PI-Ehman).

Potential competing interests: Dr Ehman owns stock in, holds intellectual property rights to, and received grants from Resoundant, Inc. Dr Sirlin consults, advises, and is on the speakers' bureau for Bayer. He received grants from GE Healthcare. The remaining authors declare no conflict of interest.

Study Highlights

WHAT IS CURRENT KNOWLEDGE

- ✓ Two-dimensional-magnetic resonance elastography (2D-MRE) is accurate in detecting advanced fibrosis in NAFLD.
- ✓ Three-dimensional-magnetic resonance elastography (3D-MRE) can evaluate a larger volume of the liver than 2D-MRE.
- ✓ No data are available regarding the diagnostic test characteristics of 3D-MRE and whether there is an advantage of evaluating a larger volume of the liver in 3D-MRE and if it further improves diagnostic test accuracy over 2D-MRE in the detection of advanced fibrosis in well-characterized patients with biopsy-proven nonalcoholic fatty liver disease (NAFLD).

WHAT IS NEW HERE

- ✓ First prospective study to show the diagnostic accuracy of 3D-MRE at various frequencies in patients with NAFLD who have a clinical indication for a liver biopsy.
- ✓ First head to head comparative study comparing 2D-MRE vs. 3D-MRE.
- ✓ 3D-MRE at 40 Hz is significantly more accurate than 2D-MRE at 60 Hz for diagnosis of advanced fibrosis in NAFLD with liver biopsy as the gold standard.

REFERENCES

1. Chalasani N, Younossi Z, Lavine JE *et al.* The diagnosis and management of non-alcoholic fatty liver disease: practice guideline by the American Association for the Study of Liver Diseases, American College of

© 2016 by the American College of Gastroenterology

Gastroenterology, and the American Gastroenterological Association. Am J Gastroenterol 2012;107:811–26.
2. Loomba R, Sanyal AJ. The global NAFLD epidemic. Nat Rev Gastroenterol Hepatol 2013;10:686–90.
3. Vernon G, Baranova A, Younossi ZM. Systemic review: the epidemiology and natural history of non-alcoholic fatty liver disease and non-alcoholic steatohepatitis in adults. Aliment Pharmacol Ther 2011;34:274–85.
4. Williamson RM, Price JF, Glancy S *et al.* Prevalence of and risk factors for hepatic steatosis and nonalcoholic fatty liver disease in people with type 2 diabetes: the Edinburgh Type 2 Diabetes Study. Diabetes Care 2011;34: 1139–44.
5. Loomba R, Abraham M, Unalp A *et al.* Association between diabetes, family history of diabetes, and risk of nonalcoholic steatohepatitis and fibrosis. Hepatology 2012;56:943–51.
6. Arulanandan A, Ang B, Bettencourt R *et al.* Association between quantity of liver fat and cardiovascular risk in patients with nonalcoholic fatty liver disease independent of nonalcoholic steatohepatitis. Clin Gastroenterol Hepatol. 2015;13:1513–20.e1.
7. Williams CD, Stengel J, Asike MI *et al.* Prevalence of nonalcoholic fatty liver disease and nonalcoholic steatohepatitis among a largely middle-aged population utilizing ultrasound and liver biopsy: a prospective study. Gastroenterology 2011;140:124–31.
8. Browning JD, Szczepaniak LS, Dobbins R *et al.* Prevalence of hepatic steatosis in an urban population in the United States: impact of ethnicity. Hepatology 2004;40:1387–95.
9. Lazo M, Hernaez R, Bonekamp S *et al.* Non-alcoholic fatty liver disease and mortality among US adults: prospective cohort study. BMJ 2011;343:d6891.
10. Adams LA, Lymp JF, St. Sauver J *et al.* The natural history of nonalcoholic fatty liver disease: a population-based cohort study. Gastroenterology 2005;129:113–21.
11. Ekstedt M, Franzen LE, Mathiesen UL *et al.* Long-term follow-up of patients with NAFLD and elevated liver enzymes. Hepatology 2006;44:865–73.
12. Guzman G, Brunt EM, Petrovic LM *et al.* Does nonalcoholic fatty liver disease predispose patients to hepatocellular carcinoma in the absence of cirrhosis? Arch Pathol Lab Med 2008;132:1761–6.
13. Matteoni CA, Younossi ZM, Gramlich T *et al.* Nonalcoholic fatty liver disease: a spectrum of clinical and pathological severity. Gastroenterology 1999;116:1413–9.
14. Ratziu V. Charlotte F, Heurtier A *et al.* Sampling variability of liver biopsy in nonalcoholic fatty liver disease. Gastroenterology 2005;128:1898–906.
15. Cadranel JF, Rufat P, Degos F.. Practices of liver biopsy in France: results of a prospective nationwide survey. For the Group of Epidemiology of the French Association for the Study of the Liver (AFEF). Hepatology 2000;32:477–81.
16. Cusi K, Chang Z, Harrison S *et al.* Limited value of plasma cytokeratin-18 as a biomarker for NASH and fibrosis in patients with nonalcoholic fatty liver disease (NAFLD). J Hepatol 2014;60:167–74.
17. Angulo P, Hui JM, Marchesini G *et al.* The NAFLD fibrosis score: a noninvasive system that identifies liver fibrosis in patients with NAFLD. Hepatology 2007;45:846–54.
18. Sterling RK, Lissen E, Clumeck N *et al.* Development of a simple noninvasive index to predict significant fibrosis in patients with HIV/HCV coinfection. Hepatology 2006;43:1317–25.
19. Guha IN, Parkes J, Roderick P *et al.* Noninvasive markers of fibrosis in nonalcoholic fatty liver disease: validating the European Liver Fibrosis Panel and exploring simple markers. Hepatology 2008;47:455–60.
20. Shah AG, Lydecker A, Murray K *et al.* Comparison of noninvasive markers of fibrosis in patients with nonalcoholic fatty liver disease. Clin Gastroenterol Hepatol 2009;7:1104–12.
21. McPherson S, Stewart SF, Henderson E *et al.* Simple non-invasive fibrosis scoring systems can reliably exclude advanced fibrosis in patients with nonalcoholic fatty liver disease. Gut 2010;59:1265–9.
22. Palmeri ML, Wang MH, Rouze NC *et al.* Noninvasive evaluation of hepatic fibrosis using acoustic radiation force-based shear stiffness in patients with nonalcoholic fatty liver disease. J Hepatol 2011;55:666–72.
23. Friedrich-Rust M, Nierhoff J, Lupsor M *et al.* Performance of Acoustic Radiation Force Impulse imaging for the staging of liver fibrosis: a pooled meta-analysis. J Viral Hepat 2012;19:e212–e219.
24. Myers RP, Pomier-Layrargues G, Kirsch R *et al.* Feasibility and diagnostic performance of the FibroScan XL probe for liver stiffness measurement in overweight and obese patients. Hepatology 2012;55:199–208.
25. Wong VW, Vergniol J, Wong GL *et al.* Liver stiffness measurement using XL probe in patients with non-alcoholic fatty liver disease. Am J Gastroenterol 2012;107:1862–71.
26. Huwart L, Sempoux C, Vicaut E *et al.* Magnetic resonance elastography for the noninvasive staging of liver fibrosis. Gastroenterology 2008;135:32–40.
27. Kim D, Kim WR, Talwalkar JA *et al.* Advanced fibrosis in nonalcoholic fatty liver disease: noninvasive assessment with MR elastography. Radiology 2013;268:411–9.
28. Loomba R, Wolfson T, Ang B *et al.* Magnetic resonance elastography predicts advanced fibrosis in patients with nonalcoholic fatty liver disease: a prospective study. Hepatology 2014;60:1920–8.
29. Le T-A, Chen J, Changchien C *et al.* Effect of colesevelam on liver fat quantified by magnetic resonance in nonalcoholic steatohepatitis: a randomized controlled trial. Hepatology 2012;56:922–32.
30. Loomba R, Sirlin CB, Ang B *et al.* Ezetimibe for the treatment of nonalcoholic steatohepatitis: assessment by novel MRI and MRE in a randomized trial (MOZART Trial). Hepatology 2015;61:1239–50.
31. Neuschwander-Tetri BA, Loomba R, Sanyal AJ *et al.* Farnesoid X nuclear receptor ligand obeticholic acid for non-cirrhotic, non-alcoholic steatohepatitis (FLINT): a multicenter, randomized, placebo-controlled trial. Lancet 2015;385:956–65.
32. Patel NS, Doycheva I, Peterson MR *et al.* Effect of weight loss on magnetic resonance imaging estimation of liver fat and volume in patients with nonalcoholic steatohepatitis. Clin Gastroenterol Hepatol 2015;13:561–8.
33. Zarrinpar A, Gupta S, Maurya MR *et al.* Serum microRNAs explain discordance of non-alcoholic fatty liver disease in monozygotic and dizygotic twins: a prospective study. Gut 2015; doi:10.1136/gutjnl-2015-309456.
34. Kleiner DE, Brunt EM, Van Natta M *et al.* Design and validation of a histological scoring system for nonalcoholic fatty liver disease. Hepatology 2005;41:1313–21.
35. Yin M, Talwalkar JA, Glaser KJ *et al.* Assessment of hepatic fibrosis with magnetic resonance elastography. Clin Gastroenterol Hepatol 2007;5: 1207–1213.e2.
36. Chen J, Talwalkar JA, Yin M *et al.* Early detection of nonalcoholic steatohepatitis in patients with nonalcoholic fatty liver disease by using MR elastography. Radiology 2011;259:749–56.
37. Venkatesh SK, Yin M, Ehman RL. Magnetic resonance elastography of liver: technique, analysis, and clinical applications. J Magn Reson Imaging 2013;37:544–55.
38. Loomba R, Schork N, Chen CH *et al.* Heritability of hepatic fibrosis and steatosis based on a prospective twin study. Gastroenterology 2015;149: 1784–93.
39. Oliphant TE, Manduca A, Ehman RL *et al.* Complex-valued stiffness reconstruction for magnetic resonance elastography by algebraic inversion of the differential equation. Magn Reson Med 2001;45:299–310.
40. Permutt Z, Le T-A, Peterson MR *et al.* Correlation between liver histology and novel magnetic resonance imaging in adult patients with non-alcoholic fatty liver disease—MRI accurately quantifies hepatic steatosis in NAFLD. Aliment Pharmacol Ther 2012;36:22–9.
41. Noureddin M, Lam J, Peterson MR *et al.* Utility of magnetic resonance imaging versus histology for quantifying changes in liver fat in nonalcoholic fatty liver disease trials. Hepatology 2013;58:1930–40.
42. Wai C-T, Greenson JK, Fontana RJ *et al.* A simple noninvasive index can predict both significant fibrosis and cirrhosis in patients with chronic hepatitis C. Hepatology 2003;38:518–26.
43. DeLong ER, DeLong EM, Clarke-Pearson DL. Comparing the areas under two or more correlated receiver operating characteristic curves: a nonparametric approach. Biometrics 1988;44:837–45.
44. Lin SC, Heba E, Wolfson T *et al.* Noninvasive diagnosis of nonalcoholic fatty liver disease and quantification of liver fat using a new quantitative ultrasound technique. Clin Gastroenterol Hepatol 2015;13:1337–1345.e6.
45. Castera L, Vilgrain V, Angulo P.. Noninvasive evaluation of NAFLD. Nat Rev Gastroenterol Hepatol 2013;10:666–75.
46. Berzigotti A, Castera L. Update on ultrasound imaging of liver fibrosis. J Hepatol 2013;59:180–2.
47. Dill T. Contraindications to magnetic resonance imaging: non-invasive imaging. Heart 2008;94:943–8.
48. Cui J, Ang B, Haufe W. Comparative diagnostic accuracy of magnetic resonance elastography vs. eight clinical prediction rules for non-invasive diagnosis of advanced fibrosis in biopsy-proven non-alcoholic fatty liver disease: a prospective study. Aliment Pharmacol Ther 2015;41:1271–80.